

Measurement of the Static Quadrupole Moments of the First 2^+ States of ^{194}Pt , ^{196}Pt , and ^{198}Pt †

J. E. GLENN,* R. J. PRYOR, AND J. X. SALADIN
University of Pittsburgh, Pittsburgh, Pennsylvania 15213
 (Received 18 July 1969)

The values of the $B(E2, 0^+ \rightarrow 2^+)$ and the static quadrupole moments of the first 2^+ states of ^{194}Pt , ^{196}Pt , and ^{198}Pt are determined. The evaluation includes a discussion of quantum-mechanical effects as well as the influence of atomic screening.

I. INTRODUCTION

IN a previous paper,¹ we described in detail the experimental determination of the quadrupole moment Q_2^+ of the first excited state of ^{114}Cd by inelastic scattering of ^{16}O ions, using higher-order effects in Coulomb excitation. It subsequently appeared interesting to apply this method to a systematic study of Q_2^+ of

TABLE I. Isotopic enrichments.

Target	Isotope	Percent present	Precision in percent
^{194}Pt	192	0.2	...
	194	65.7	± 0.2
	195	28.6	± 0.2
	196	5.6	± 0.1
	198	0.4	...
^{196}Pt	190	0.1	
	192	0.1	
	194	8.91	± 0.1
	195	33.46	± 0.1
	196	54.89	± 0.1
	198	2.74	± 0.1
^{198}Pt	190	0.1	
	192	0.1	
	194	4.94	± 0.1
	195	11.54	± 0.1
	196	26.70	± 0.1
	198	56.82	± 0.1

nuclei just above and below the region, $150 < A < 190$, of permanent deformation. Here, we present the results of such measurements on the isotopes $^{194,196,198}\text{Pt}$. A preliminary report has been published earlier.² The evaluation presented here includes a discussion of quantum-mechanical effects as well as the influence of atomic screening. In Sec. III, the results are compared with various theoretical predictions.

† Work supported by the National Science Foundation.

* Present address: Nuclear Physics Laboratory, University of Colorado, Boulder, Colo. 80302.

¹ J. X. Saladin, J. E. Glenn, and R. J. Pryor (unpublished).

² J. E. Glenn and J. X. Saladin, Phys. Rev. Letters **20**, 1298 (1968).

II. EXPERIMENTAL PROCEDURE AND DATA EVALUATION

The experiment was carried out with 42-MeV ^{16}O ions and 6-MeV protons from the Pittsburgh Tandem Van de Graaff. The scattered ions were energy analyzed by means of an Enge split-pole spectrograph. The experimental procedures and data analysis were identical to those discussed in Ref. 1. The targets were prepared by vacuum evaporation of the isotopically enriched material onto $10\text{-}\mu\text{g}/\text{cm}^2$ carbon backings, using a Varian electron gun. The targets varied in thickness

TABLE II. Experimental ratios $R_{\text{expt}} = d\sigma_{2^+}/d\sigma_{\text{el}}$.

Isotope	Lab angle	Beam energy (MeV)	R_{expt}
^{194}Pt	44.4°	42 (^{16}O)	0.00422 ± 0.00005
	59.4°	42	0.01034 ± 0.00014
	89.4°	42	0.02925 ± 0.00041
	119.4°	42	0.05237 ± 0.00065
	143.4°	42	0.06726 ± 0.00060
	143.4°	6 (protons)	0.00127 ± 0.00001
^{196}Pt	44.4°	42	0.00364 ± 0.00006
	89.4°	42	0.02537 ± 0.00061
	143.4°	42	0.0563 ± 0.0011
^{198}Pt	44.4°	42	0.00226 ± 0.00004
	75.0°	42	0.01025 ± 0.00013
	89.4°	42	0.01723 ± 0.00034
	143.4°	42	0.03514 ± 0.00070

from between 5 to $15\ \mu\text{g}/\text{cm}^2$. Some typical ^{16}O spectra are shown in Fig. 1. The energy resolution varied from between 70- and 100-keV full width at half-maximum (FWHM), depending on target thickness and scattering angle. The ratios $R_{\text{expt}} = d\sigma_{\text{inel}}(2^+)/d\sigma_{\text{el}}$ were extracted from the data after contributions from isotopic impurities had been subtracted. The subtractions were made using the Oak Ridge isotopic analysis shown in Table I. Since the available isotopic enrichments were rather poor, a consistent peak-shape-analysis computer program (GROPE) was developed. The program is based on two assumptions: (1) The amount of contaminant present is known, relative to the main isotope.

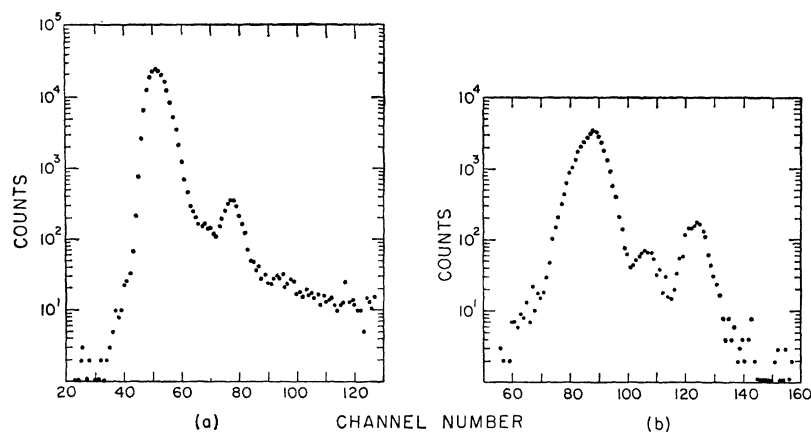


FIG. 1. (a) Spectrum for scattering of 42-MeV ^{16}O ions from ^{198}Pt . $\theta_{\text{lab}}=75^\circ$. (b) Spectrum for scattering of 42-MeV ^{16}O ions from ^{194}Pt . $\theta_{\text{lab}}=143.4^\circ$. The middle peak is due to ^{196}Pt .

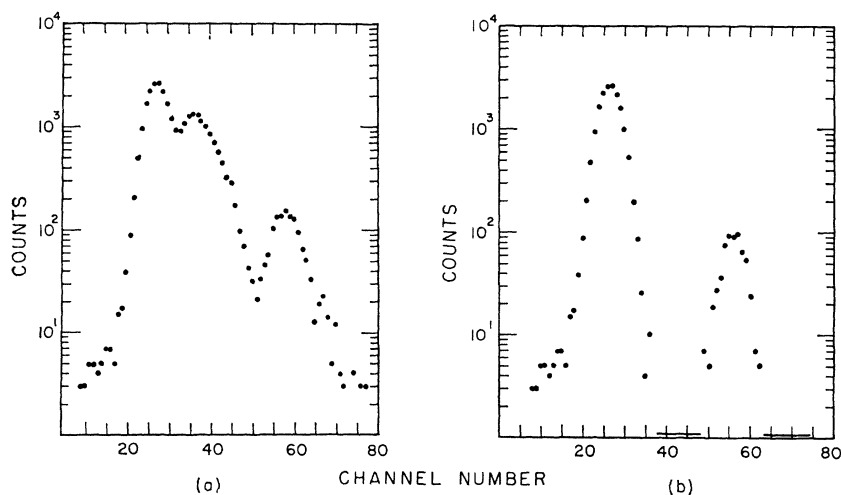


FIG. 2. (a) Spectrum for scattering of 42-MeV ^{16}O ions from ^{198}Pt . $\theta_{\text{lab}}=143.4^\circ$. (b) The same spectrum after peak-shape analysis as described in the text.

TABLE III. Input information for Pt^{194} calculations.

Level index n	Excitation energy (MeV)	Spin and parity	M_{1n}	Matrix elements			M_{4n}
				M_{2n}	M_{3n}		
1	0.000	0^+	0	M_{21}	± 0.093		0
2	0.328	2^+	M_{12}	M_{22}	± 1.07		± 2.062
3	0.622	2^+	$+0.093$	± 1.07	0		0
4	0.811	4^+	0	$+2.062$	0		0

TABLE IV. Input information for Pt^{196} calculations.

Level index n	Excitation energy (MeV)	Spin and parity	M_{1n}	Matrix elements			M_{4n}
				M_{2n}	M_{3n}		
1	0.000	0^+	0	M_{21}	$+0.036$		0
2	0.356	2^+	M_{12}	M_{22}	± 0.012		$+1.844$
3	0.689	2^+	$+0.036$	$+0.012$	0		0
4	0.877	4^+	0	$+1.844$	0		0

(2) The shape is the same for all peaks. At back angles, the elastic peaks due to different isotopes were often sufficiently well separated to permit cross checks on the isotopic-abundance figures supplied by Oak Ridge. The results of such checks were always consistent with the Oak Ridge data and thus justify assumption (1). Assumption (2) was checked experimentally by placing monoisotopic elastic peaks at different locations on the position-sensitive detector. The widths (FWHM) of these peaks were found to vary by less than 5% and errors due to these variations were estimated to be negligible.

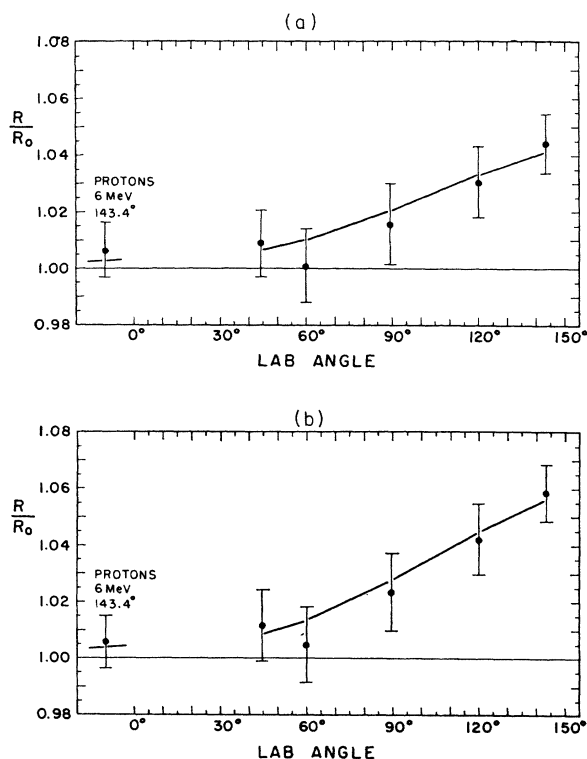


FIG. 3. Results of the least-square-fit analysis for ^{194}Pt . (a) Sign of the product $(M_{12}M_{23}M_{13}M_{22})$ positive. (b) Sign of the product $(M_{12}M_{23}M_{13}M_{22})$ negative.

The program input includes the percentages of each contaminant present, the positions of all peaks (as determined from an energy calibration), a trial peak shape, and the experimental spectrum. First, contaminant peaks are subtracted using the trial shape, then the shape of the main elastic peak which remains after contaminants are subtracted is compared to the trial shape, and a new trial shape is chosen as a compromise between the two shapes. The procedure is repeated until the difference between trial shape and remaining elastic peak becomes negligibly small. The resultant spectrum after the contaminant peaks have been subtracted is obtained as computer output. Figure 2(a)

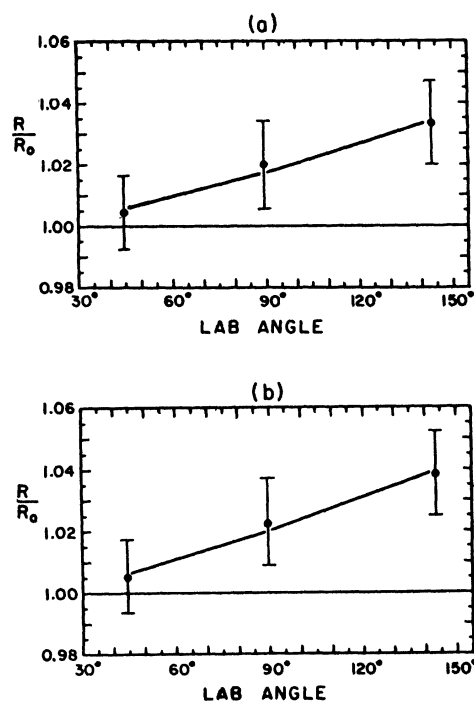


FIG. 4. Results of least-square analysis for ^{196}Pt . (a) Sign of the product $(M_{12}M_{23}M_{13}M_{22})$ positive. (b) Sign of the product $(M_{12}M_{23}M_{13}M_{22})$ negative.

shows as an example an experimental spectrum while Fig. 2(b) shows the same spectrum after the subtraction procedure.

The experimental ratios R_{expt} are shown in Table II. These ratios were compared with computer calculations³ in which the electric quadrupole matrix element

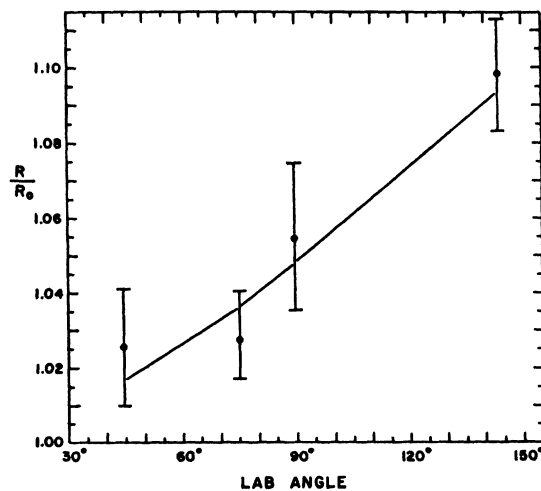


FIG. 5. Least-square analysis for ^{198}Pt .

³ A. Winther and J. de Boer, in *Coulomb Excitation*, edited by K. Alder and A. Winther (Academic Press Inc., New York, 1966).

TABLE V. Input information for Pt¹⁹⁸ calculations.

Level index <i>n</i>	Excitation energy (MeV)	Spin and parity	Matrix elements	
			M_{1n}	M_{2n}
1	0.000	0 ⁺	0	M_{21}
2	0.408	2 ⁺	M_{12}	M_{22}

M_{12} between the ground state and the first excited state, and the diagonal matrix element M_{22} of the first excited states were treated as variable parameters. The information about the nuclear states included in the computer calculations is shown in Tables III–V. Fits obtained from a least-squares analysis are shown in Figs. 3–5, where the quantity $q = R/R_0$ is displayed as a function of the scattering angle. R_0 is the calculated ratio $d\sigma_{inel}/d\sigma_{el}$ assuming $Q_2^+ = 0$. For the ¹⁹⁴Pt and ¹⁹⁶Pt isotopes, fits were obtained for both possible signs of the product ($M_{12}M_{22}M_{13}M_{23}$). The theory of Kumar and Baranger, which is discussed below, predicts that this product is negative. This corresponds to the larger Q_2^+ values listed in Table VI which summarizes the results of the least-squares analysis. The errors shown include estimates of systematic errors due to impurity and background subtractions and virtual excitation via the giant-dipole resonance. Column 5 contains for comparison the $B(E2)$ values of Milner *et al.*,⁴ which are systematically higher than ours. Their data were calculated under the assumption $Q_2^+ = 0$. Including Q_2^+ in the evaluation lowers the $B(E2)$ values of Ref. 4 by about 6% and the two sets of data are then consistent within the quoted errors.

The quantum-mechanical effects were estimated in the same manner as in Ref. 1, using the results of Alder and Pauli.⁵ The thus corrected quadrupole moments are given in column 8 of Table VI and are about 4% higher than the semiclassical values.

The effect due to electronic screening was also discussed in Ref. 1. In the present case, it amounts to an increase in the effective bombarding energy of 115 keV

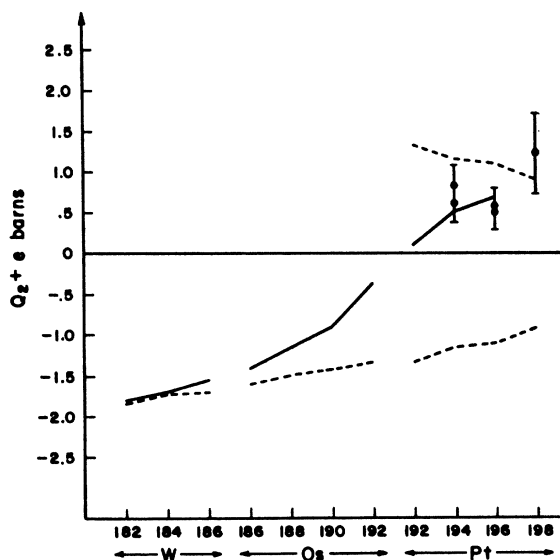


FIG. 6. Comparison between experimentally determined quadrupole moments and various mode predictions.

which results in a lowering of the $B(E2)$ values by 0.8%. These corrected values are shown in column 4 of Table VI.

III. DISCUSSION

In Fig. 6, the results of the quadrupole moment measurements are summarized and compared with the predictions of various models in the W–Os–Pt region. The most remarkable features of the experimental data are (1) the magnitude of Q_2^+ which represents several single-particle units, and (2) the positive sign of Q_2^+ which is opposite to that found in the region of permanent deformation. The most ambitious calculation in this region is that of Kumar and Baranger,⁶ which is quite successful in predicting the excitation spectrum. Recent measurements by Casten *et al.*⁷ and Milner *et al.*⁴ on the electromagnetic properties of these nuclei (transition rates, branching ratios, etc.) showed that the Kumar-Baranger theory predicts the general trend

TABLE VI. Summary of results and comparison with the calculation of Kumar and Baranger (KB).

Isotope	Sign of $M_{12}M_{22}M_{13}M_{23}$	Present work	$B(E2, 0^+, 2^+) (e^2 b^2)$			Q_2^+ (e b)	Q_2^+ including correction	Q_2^+ in the KB theory ^b
			Corrected per screening	Milner <i>et al.</i> ^a	KB theory			
¹⁹⁴ Pt	+	1.65±0.04	1.64±0.04			0.62±0.16	0.64±0.16	
¹⁹⁴ Pt	–	1.65±0.04	1.64±0.04	1.93±0.17	1.70	0.84±0.18	0.87±0.18	0.492
¹⁹⁶ Pt	+	1.50±0.05	1.49±0.05			0.49±0.18	0.51±0.18	
¹⁹⁶ Pt	–	1.50±0.05	1.49±0.05	1.63±0.15	1.43	0.56±0.18	0.58±0.18	0.699
¹⁹⁸ Pt	0	1.01±0.05	1.01±0.05	1.22±0.11		1.22±0.5		

^a See Ref. 4.^b See Ref. 6.⁴ W. T. Milner, F. K. McGowan, R. L. Robinson, P. H. Stelson, and R. D. Sayer, *Bull. Am. Phys. Soc.* **12**, 1201 (1967).⁵ K. Alder and H. K. A. Pauli, *Nucl. Phys.* **A128**, 1 (1969).⁶ K. Kumar and H. Baranger, *Nucl. Phys.* **A122**, 273 (1968).⁷ R. F. Casten, J. S. Greenberg, G. A. Buginyon, and D. A. Bromley, *Phys. Rev. Letters* **18**, 912 (1967).

of the experimental results quite well. Starting point of the theory is Bohr's collective Hamiltonian. The six kinetic-energy functions and the potential-energy function which enter into the Hamiltonian are derived from the pairing-plus-quadrupole model of residual interactions. The Hamiltonian is then diagonalized exactly by a numerical method. The solid curve in Fig. 6 is drawn through the predictions of this theory. The higher experimental points correspond to the theoretical prediction for the sign of the interference term. Within the experimental error, the agreement between experiment and theory is quite remarkable, especially as to the sign of Q_2^+ . Measurements on the isotopes of Os which are in progress⁸ confirm the predicted change in the sign of Q_2^+ in this region.

⁸ R. J. Pryor, J. X. Saladin, J. R. Kerns, and S. Lane, *Bull. Am. Phys. Soc.* **14**, 123 (1969).

The dashed line is drawn through values obtained from the symmetric-rotor-model relation

$$(M_{22}/M_{12})^2 = 10/7$$

using experimental values for M_{12} .

ACKNOWLEDGMENT

It is a pleasure to acknowledge stimulating discussions and correspondence with Professor K. Alder, Professor M. Baranger, Dr. K. Kumar, and Dr. H. Pauli. We are very much indebted to J. R. Kerns and Dr. P. Crowley for extensive help in accumulating and analyzing the data. One of us (J.X.S.) is very grateful for the hospitality of the Physics Department of the University of Basel where part of this paper was written.

Prompt K X Rays as a Function of Fragment Mass and Total Kinetic Energy in the Thermal Fission of U^{235} †*

E. M. BOHN,† B. W. WEHRING, AND M. E. WYMAN

Nuclear Engineering Program, University of Illinois, Urbana, Illinois 61801

(Received 11 August 1969)

In order to obtain information about the deexcitation of fission fragments and the division of nuclear charge in fission for the case of thermal-neutron fission of U^{235} , a measurement of the prompt K x rays (0 to ~ 1 nsec after fission) was performed. A thin foil of uranium was caused to fission by a beam of neutrons from a beam port of a nuclear reactor. The fission fragments were detected by silicon surface-barrier detectors, and the x rays, by a NaI(Tl) scintillator. A three-parameter analyzer recorded the energies of the two fragments and the energy of the x ray emitted in coincidence with the fragments. The x-ray energies were sorted "off line" according to fragment mass or total kinetic energy in order to obtain x-ray spectra for different mass groups and different energy groups. From these spectra, x-ray yields were found as a function of fragment mass and as a function of total kinetic energy of the fragments. The results are compared, where possible, with those obtained in other laboratories for the thermal-neutron fission of U^{235} and with results for the spontaneous fission of Cf^{252} . Differences and similarities are noted. The most probable charge versus mass was also estimated from the spectra, and these results are in agreement with radiochemical analysis.

I. INTRODUCTION

RECENTLY, a great deal of interest has developed in the study of K x rays emitted by excited fission fragments. The interest has been stimulated by the fact that such studies lead to information about the charge division in fission. Also of importance is the information about fragment deexcitation processes found by the investigations.

Many studies of the K x rays coincident with the

spontaneous fission of Cf^{252} have been performed.¹⁻⁶ Glendenin and Griffin¹ reported that a total of $0.55 \pm 0.05K$ x rays per fission were emitted between 0 and ~ 0.3 μ sec after fission, and that the times of emission were characteristic of the internal conversion process. Further studies^{2-4,6} showed that for various time intervals after fission, K x-ray yields per fragment depend on fragment mass. More recently, high-

¹ L. E. Glendenin and H. C. Griffin, *Phys. Letters* **15**, 153 (1965).

² L. E. Glendenin and J. P. Unik, *Phys. Rev.* **140**, B1301 (1965).

³ S. S. Kapoor, H. R. Bowman, and S. G. Thompson, *Phys. Rev.* **140**, B1310 (1965).

⁴ R. A. Atneosen, T. D. Thomas, W. M. Gibson, and M. L. Perlman, *Phys. Rev.* **148**, 1206 (1966).

⁵ R. L. Watson, H. R. Bowman, and S. G. Thompson, *Phys. Rev.* **162**, 1169 (1967).

⁶ A. B. Long, B. W. Wehring, and M. E. Wyman, *Phys. Rev.* **188**, 1948 (1969).

† The work reported in this article was supported by the National Science Foundation.

* The material in this article is based upon a dissertation by one of the authors (EMB) submitted in partial fulfillment of the requirements for the doctoral degree at the University of Illinois.

‡ Present address: Reactor Physics Division, Argonne National Laboratory, Argonne, Ill.